Table DR1
Table DR2A, Table DR2B, Table DR2C
Table DR3
Table DR4

Sample Collection and Analysis

Sampling occurred by hand during the dry seasons of 2005-09 and 2012, whereas wet season sampling occurred from 2005-07 and in 2011. Individual sites were sampled between 1-11 times. Care was taken to collect pristine samples from fast-moving parts of streams and from rivers upstream of any local anthropogenic activity.

Waters were analyzed for major ion contents at OSU. Cation abundances were measured using either ion chromatography (IC) or inductively-coupled plasma-optical emission spectrometry (ICP-OES) and anion concentrations determined by IC analysis. Silica contents were measured by ICP-OES. IC analysis utilized Dionex^{TM} DX-120 ion exchange resin and followed the procedures described in Welch et al. (2010). Precision of all measurements was usually 5% or better. Accuracy of the samples analyzed by ICP-OES was checked against an independent standard (NIST Standard Reference Material 1643e).

Derived Parameters

Bicarbonate (HCO_3^-) was calculated from the measured cation-anion difference by subtracting the total anion equivalents from cation equivalents ($\Sigma mEq_{cations} - \Sigma mEq_{anions}$) following Lyons et al. (2005). Because of slight differences in multimeter calibration from one field campaign to another over the nine years of the project, TDS was also calculated from the sum of cation and anion abundances as follows:

$$TDS_{(c)}\ mg/L = Na^+ + K^+ + Mg^{2+} + Ca^{2+}, + HCO_3^-, + Cl^-, + SO_4^{\ 2} + NO_3^-, \qquad \text{Eq. 1}$$

which is used throughout the discussion that follows unless otherwise indicated.

There is an excess of Na over Cl in almost all Panama waters. Excluding the streams and rivers developed on Tertiary marine sediments in the Burica peninsula and Trans-Isthmus region, which are strongly enriched in both Na^+ and Cl^-, the surplus Na^+ to Cl^-, present in waters draining the magmatic arc represents the Na contribution from silicate weathering. Therefore, the 'seasalt' component was quantified following Murphy and Stallard (2012), assuming that all Cl^- in the Panama waters sampled was "cyclic" in origin (Keene et al., 1986) and that other elemental constituents were not fractionated during vapor formation or transport,. The species-to-chloride ratios used for this adjustment were: $Na^+/Cl^- = 0.85251$, $K^+/Cl^- = 0.01790$, $Mg^{2+}/Cl^- = 0.09689$, $Ca^{2+}/Cl^- = 0.01879$, and $SO_4^{2-}/Cl^- = 0.052$. The seasalt contribution was subtracted from measured Na^+, K^+, Mg^{2+}, Ca^{2+}, and SO_4^{2-} concentrations to estimate the solute input from bedrock weathering..

Physical Erosion Rates

Long-term physical erosion rates are taken from Sosa-Gonzalez et al. (2011). Stream sediments were collected in 2004, 2007, and 2009 and subsequently shipped to the Mineral Separation Laboratory at the University of Vermont for preparation. The samples were dried and sieved, and the 250-850 μm grain size was isolated and treated chemically treated to isolate quartz and extract ^{10}Be using the methodology of Kohl and Nishiizumi (1992). Isotopic ratios measurements were made using Accelerator Mass Spectrometry (AMS) at Lawrence Livermore National Laboratory. Finally, erosion rates were subsequently calculated from the isotopic data using the CRONUS Earth Calculator (http://hess.ess.washington.edu/).

Flux Calculation Methodology

Cation and silicate fluxes and CO_2 consumption values were calculated using a subset of 62 samples from two regions -35 grab samples from five rivers of the Greater Panama Canal Watershed collected during 2005-09 and 27 grab samples from 14 rivers draining the Cordillera Central in Chiriqui, Veraguas and Cocle provinces collected during 2006-07. The dataset was corrected for precipitation after Murphy and Stallard (2012) and for non-silicate contribution of Ca and Mg using andesite end-member ratios of 0.5 for Ca/Na and Mg/Na of Gaillardet et al. (1999) prior to its use in calculations. A multi-step process was employed whereby individual cation compositions were first multiplied by the average daily discharge value from gauging stations of either the Empresa de Transmisión Eléctrica or Autoridad del Canal de Panama to produce an instantaneous denudation flux. Plots comparing the instantaneous denudation fluxes with respective discharge values were then compiled to produce specific elemental flux determination equations. High r^2 values support this approach for moles (Ca=0.88; Mg=0.92; Na=0.92; K=0.80; and Si=0.96; and tons (Ca=0.92; Mg=0.92; Na=0.92; K=0.80; and Si=0.96, respectively (Fig S1 & S2). Finally, long-term monthly discharge values were substituted into the equations and calculated denudation values divided by watershed area to produce cation and silicate weathering yields for 36 rivers. CO_2 consumption was calculated by dividing the precipitation and silicate corrected Na+K+Mg(2x)+Ca(2x) annual flux values by watershed area.

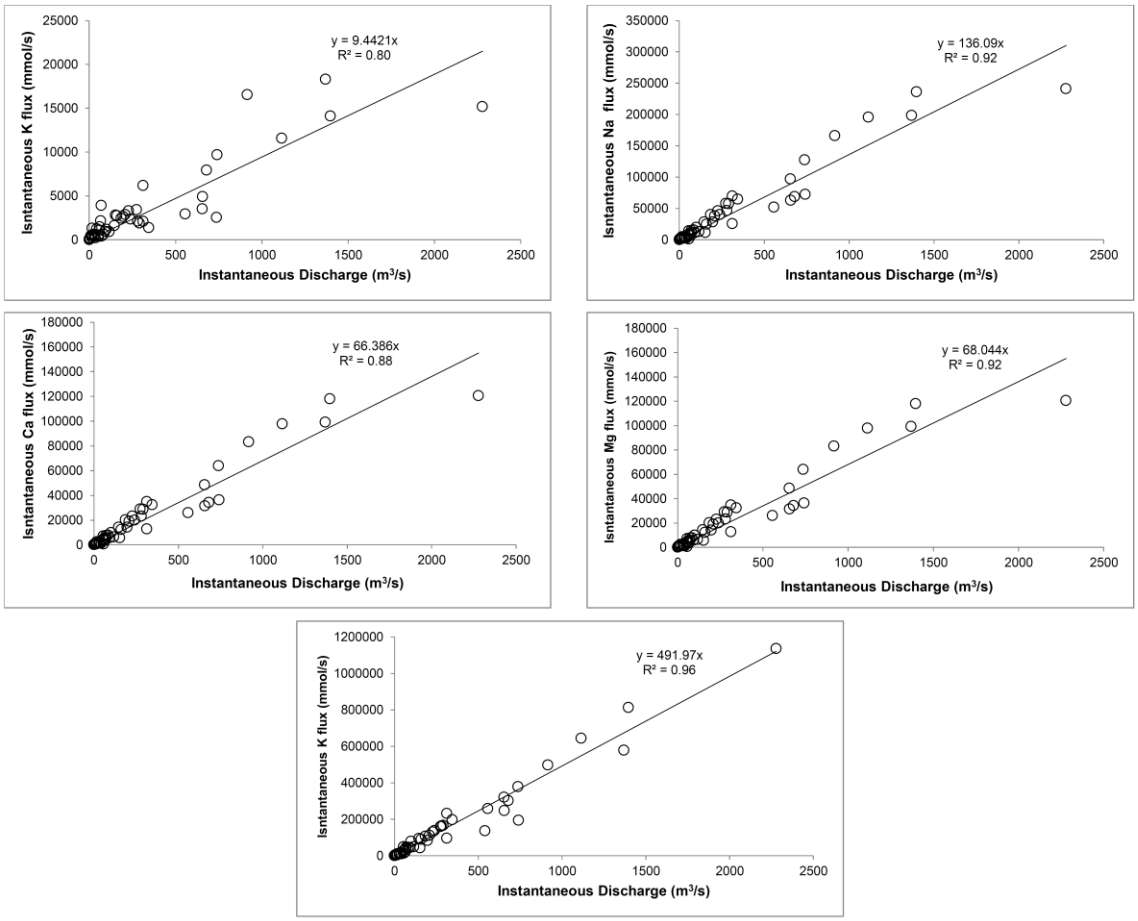

Figure S1. Correlation plots for comparisons of instantaneous elemental fluxes (in mmol/s) versus instantaneous discharge (m^3/s).

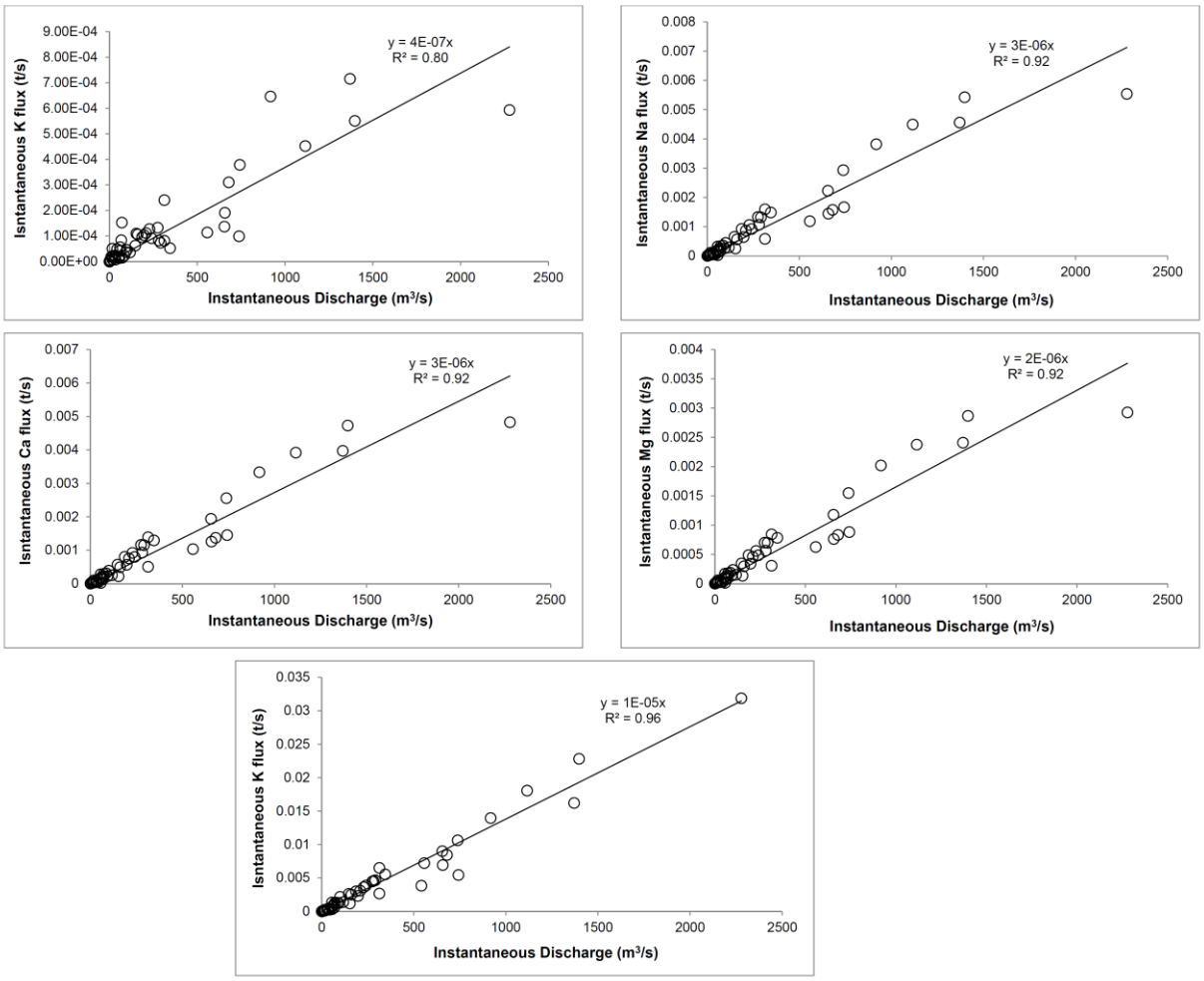

Figure S2. Correlation plots for comparisons of instantaneous elemental fluxes (in tons/s) versus instantaneous discharge (m^3/s).

GIS Analysis

A digital elevation model (DEM) for the Panama watersheds was prepared to evaluate the control of landscape geomorphology, land use practices, and climate on river chemistry and weathering fluxes. The DEM from which the Panama physiographic and watershed maps were produced is a product of the 3 arc-seconds (90m) resolution, void filled data set (Farr et al., 2007) of the NASA Jet Propulsion Laboratory's Shuttle Radar Topography Mission (SRTM) that has been processed by the National Geospatial-Intelligence Agency (NGA) (https://lta.cr.usgs.gov/SRTM). The DEM was used to elucidate river courses and define watershed boundaries, from which upstream area, stream gradient, river length and geomorphic properties were determined for each watershed. An iterative process of sink detection and filling was used to create a depression-free DEM from the SRTM DEM (Fig S3). Flow direction was

computed using the depression-free DEM, from which flow accumulation was then calculated. Next, a vector stream network was generated from the flow accumulation raster and the sampling points snapped to the streams. The sampling points were then used as the pour points to compute the watersheds from the flow direction raster. Average values of annual low and high temperature together with annual minimum and maximum precipitationvalues were determined for each watershed using data obtained from the ESRI ArcAtlas™ (http://gcmd.nasa.gov/records/GCMD_ESRI_Arc_Atlas.html). Finally, land use cover was also incorporated into the DEM using data provided by the European Space Agency's Global Land Cover Map™ (http://due.esrin.esa.int/globcover/).

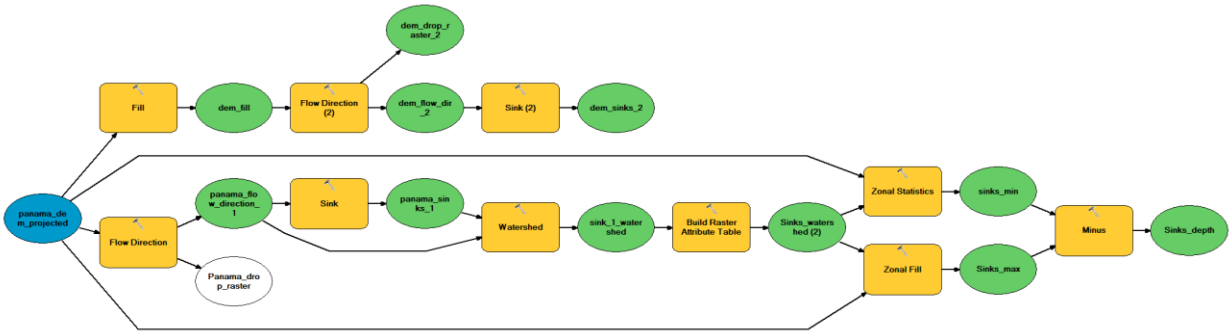

Fig S3. Geoprocessing model for computing the depression-free DEM.

Our review of the global land cover dataset revealed a total of 23 land use categories in our study area: 11 - Irrigated croplands, 14 - Rainfed croplands, 20 - Mosaic croplands / vegetation, 20 - Mosaic vegetation / croplands, 40 - Closed to open broadleaved deciduous forest, 50 - Closed broadleaved deciduous forest, 60 - Open broadleaved deciduous forest, 70 - Closed needleleaved evergreen forest, 90 - Open needleleaved deciduous or evergreen forest, 100 - Closed to open mixed broadleaved and needleleaved forest, 110 - Mosaic forest-shrubland / grassland, 120 - Mosaic Grassland / forest-shrubland, 130 - Closed to open shrubland, 140 - Closed to open grassland, 150 - Sparse vegetation, 160 - Closed to open broadleaved forest regularly flooded (fresh-brackish water), 170 - Closed broadleaved forest permanently flooded (saline brackish water), 180 - Closed to open vegetation regularly flooded, 190 - Artificial areas, 200 - Bare areas, 210 - Water bodies, 220 - Permanent snow and ice, and 230 - No data.

In order to facilitate the comparison of land use practices with silicate weathering rates, we reclassified/re-categorized the values as follows:

Class 1: Forest = 40, 50, 60, 70, 90, & 100

Class 2: Agricultural Land = 11, 14, & 20 (both types)

Class 3: Shrubland/Grassland = 110, 120, 130, & 140

Class 4: Open Land = 150 & 200

Class 5: Water Bodies = 210

Null: 160, 170, 180, 190, 220, & 230

Statistical Analysis

A Pearson correlation analysis was performed between our calculated silicate weathering fluxes and climatic, land use cover, and geomorphological parameters using SAS 9.1.3 SP4. The associated correlation plots are provided in Figure S4.

References

Farr, T.G., Rosen, A.R., Caro, E., Crippen, R., Duren, R., Hensley, S., Kobrick, M., Paller, M., Rodriguez, E., Roth, L., Seal, D., Shaffer, S., Shimanda, J., Umland, J., Werner, M., Oskin, M., Burbank, D., and Alsdorf, D., 2007, The Shuttle Radar Topography Mission: Reviews in Geophysics, v. 45, RG2004, doi:10.1029/2005RG000183.

Horwitz, E.P., Chiarizia, R., and Dietz, M.L., 1992, A novel strontium-selective extraction chromatographic resin: Solvent Extraction and Ion Exchange, v. 10, p. 313-336.

Keene, W.C., Pszenny, A.A.P., Galloway, J.N. and Hawley, M.E., 1986, Sea-salt corrections and interpretation of constituent ratios in marine precipitation: Journal Geophysical Research, v. 91, p. 6647– 6658.

Kohl, C.P., and Nishiizumi, K., 1992, Chemical Isolation of Quartz for Measurement of in-Situ Produced Cosmogenic Nuclides: Geochimica et Cosmochimica Acta, v. 56, p. 3583-3587.

Lyons, W.B., Carey, A.E., Hicks, D.M., and Nezat, C., 2005. Chemical weathering in high-sediment-yielding watersheds, New Zealand: Journal of Geophysical Research, v. 110, p. 1-11.

Murphy, S.F. and Stallard, R.F., eds., 2012, Water quality and landscape processes of four watersheds in eastern Puerto Rico: U.S. Geological Survey Professional Paper 1789, 292 p.

Sosa-Gonzales, V., Bierman, P.R., Nichols, K.K, and Rood, D.H., 2011, Determining long term erosion rates in Panama- An application of ^{10}Be: Geological Society of America *Abstracts with Programs*, v.43, p. 274.

Welch, K. A., Lyons, W. B., Whisner, C., Gardner, C. B., Gooseff, M. N., McKnight, D. M., and Priscu, J. C., 2010, Spatial variations in the geochemistry of glacial meltwater streams in the Taylor Valley, Antarctica: Antarctic Science, v. 22, p. 662–672..

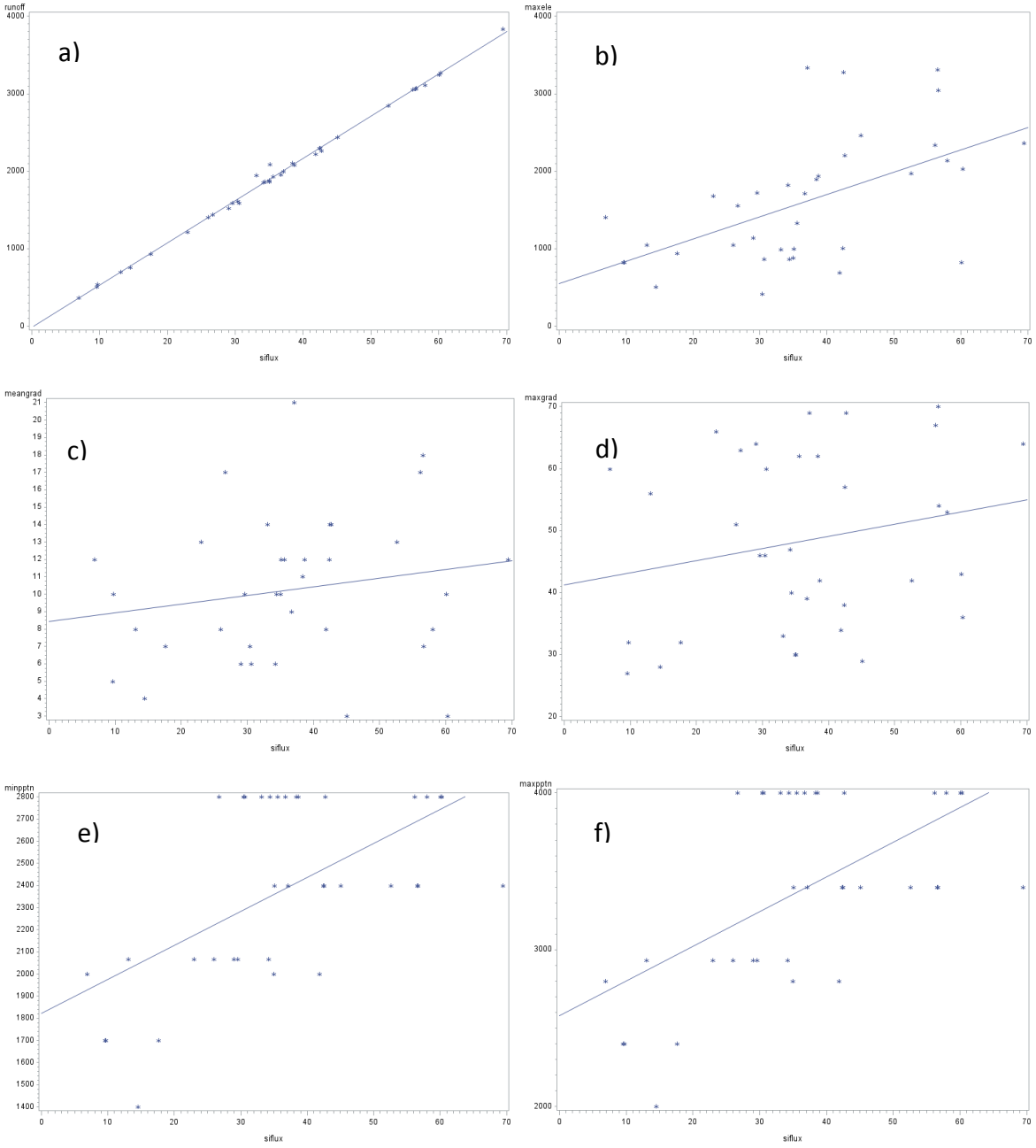

Fig S4. Pearson correlation analysis was performed between our calculated silicate weathering fluxes and: a) mean annual runoff (mm yr-1), b) maximum elevation (m), c) maximum gradient, d) mean gradient, e) minimum mean annual precipitation (mm), and f) maximum annual precipitation (mm).

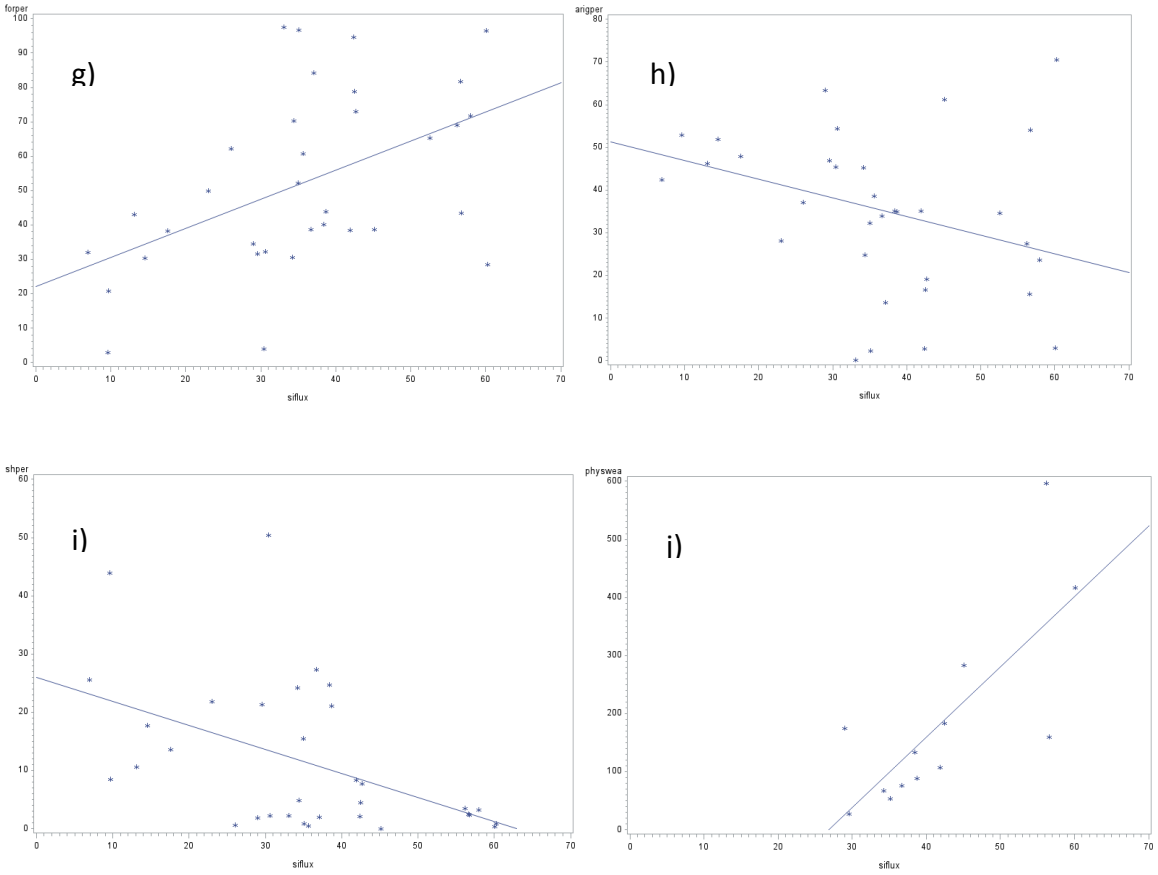

Fig S4 (cont'd.). Pearson correlation analysis was performed between our calculated silicate weathering fluxes and: g) % forest cover, h) % agricultural cover, i) % shrub/grassland cover, and j) previously determined long-term physical erosion rates.